

# Efficiently Charting RDF

Oren Kalinsky  
Technion  
Haifa, Israel

Oren Mishali  
Technion  
Haifa, Israel

Aidan Hogan  
University of Chile  
Santiago, Chile

Yoav Etsion  
Technion  
Haifa, Israel

Benny Kimelfeld  
Technion  
Haifa, Israel

## ABSTRACT

We propose a visual query language for interactively exploring large-scale knowledge graphs. Starting from an overview, the user explores bar charts through three interactions: class expansion, property expansion, and subject/object expansion. A major challenge faced is performance: a state-of-the-art SPARQL engine may require tens of minutes to compute the multiway join, grouping and counting required to render a bar chart. A promising alternative is to apply approximation through online aggregation, trading precision for performance. However, state-of-the-art online aggregation algorithms such as Wander Join have two limitations for our exploration scenario: (1) a high number of rejected paths slows the convergence of the count estimations, and (2) no unbiased estimator exists for counts under the distinct operator. We thus devise a specialized algorithm for online aggregation that augments Wander Join with exact partial computations to reduce the number of rejected paths encountered, as well as a novel estimator that we prove to be unbiased in the case of the distinct operator. In an experimental study with random interactions exploring two large-scale knowledge graphs, our algorithm shows a clear reduction in error with respect to computation time versus Wander Join.

## 1 INTRODUCTION

A variety of prominent knowledge graphs have emerged in recent years, including DBpedia [17], Freebase [18], Wikidata [75], and YAGO [44] covering multiple domains, LinkedGeoData [13] for geographic data, LinkedMDB [26] for movie information, and LinkedSDMX [23] for financial and geopolitical data. A number of companies have also announced the creation of proprietary knowledge graphs to power a variety of end-user applications, including Google,<sup>1</sup> Microsoft,<sup>2</sup> Amazon<sup>3</sup> and eBay<sup>4</sup>, among others.

<sup>1</sup><https://googleblog.blogspot.com/2012/05/introducing-knowledge-graph-things-not.html>

<sup>2</sup><https://blogs.bing.com/search-quality-insights/2017-07/bring-rich-knowledge-of-people-places-things-and-local-businesses-to-your-apps>

<sup>3</sup><https://blog.aboutamazon.com/innovation/making-search-easier>

<sup>4</sup><https://www.ebayinc.com/stories/news/cracking-the-code-on-conversational-commerce/>

Due to their scale and diversity, a major challenge faced when considering a knowledge graph is to understand what content it contains: what sorts of entities it describes, what sorts of relations are represented, how extensive the coverage of particular domains is, etc. Prominent knowledge graphs, such as DBpedia [17], Freebase [18], Wikidata [75], contain in the order of tens of millions of nodes and billions of edges represented using thousands of classes and properties, spanning innumerable different domains. While a variety of approaches have been proposed to summarize or profile the content of such graphs [31], the general trend is towards either computing statistics and summaries offline, or relying on off-the-shelf query engines.

In this paper, we propose a conceptual approach and techniques for interactive exploration of large-scale knowledge graphs through a visual query language. This query language captures user interactions that follow Shneiderman’s principle for effective data visualization and exploration: “*overview first, zoom and filter, then details-on-demand*” [69]. The result of a query is a bar chart over a set of focus nodes that are defined iteratively by the user via three interactions: *class expansion*, which focuses on the sub-classes of a selected class bar, *property expansion*, which focuses on the properties defined on instances of a class, and *subject/object expansion*, which focuses on entities in the source/target of a given property. At each stage, the focus nodes of the current bar chart can be filtered by a search condition. Each interaction constitutes a visual exploration step, with the sequence of interactions captured by the query language.

Given the size and diversity of prominent knowledge graphs, the number of (intermediate) results that can be generated by queries, and the goal of supporting interactive exploration, a major challenge faced is that of performance. In preliminary experiments with Virtuoso [32]—a state-of-the-art SPARQL query engine—we found, for example, that computing the distribution of properties over all nodes in DBpedia takes over 5 minutes; such runtimes preclude the possibility of interactive exploration.

To face the critical performance problem, we investigate two orthogonal approaches. First, we explore the deployment of a query engine from the recent breed of *worst-case*

*optimal* join algorithms [57], in order to avoid an explosion of intermediate results when processing multiway joins over large graphs; for these purposes, we select the Cache Trie Join algorithm [47] to evaluate queries. Second, with the intuition that precise counts are not always required, we explore *online aggregation* algorithms [42] that trade precision for performance, computing approximate counts at a fraction of the cost observed even in the worst-case optimal setting; for these purposes, we select the Wander-Join algorithm [51]. In essence, Wander Join applies a random walk between database tuples that (jointly) match the join query, and upon termination, updates an estimator of the aggregate function.

Ultimately, we conclude that these two approaches are complementary, and we propose a novel hybrid algorithm that combines the best of both. The general idea to apply the random walk of Wander Join, and at each step, consider replacing the remaining walk with a precise computation of the space of possible suffixes, this time using Cached Trie Join. This consideration is done via an estimate of selectivity. The estimator needs to be updated accordingly, and we prove that it remains unbiased. Furthermore, we extend our algorithm to estimate counts in the presence of the distinct operator, which is crucial to our exploration use case. We call the resulting algorithm Audit Join, and prove that it provides unbiased estimators of counts, with and without the distinct operator. In experiments that evaluate randomly-generated exploration queries over two knowledge graphs, we show that our algorithm dramatically reduces error with respect to the computation time when compared with Wander Join.

## Contributions

Our contributions are summarized as follows.

- We propose a formal model of an exploration approach over knowledge graphs.
- We describe a system implementation of the exploration model.
- We devise Audit Join—a specialized online-aggregation algorithm for the backend of our proposed model, and prove that it produces unbiased estimations of counts.
- We describe an experimental study of performance over random explorations, showing the benefits of Audit Join over the state of the art.

## 2 RELATED WORK

We now give an overview of related work, focusing on two aspects: exploration tools for knowledge graphs, and relevant algorithms for query evaluation.

### Exploration Tools

A variety of approaches have been proposed in recent years for exploring and visualizing graph-structured data [28].

*Faceted Browsing:* Among the most popular approaches that have been studied for exploring knowledge graphs is that of *faceted browsing*, where users incrementally add restrictions – called *facets* – to restrict the current results [72]. Early works mainly focused on smaller, domain-specific graphs, among which we mention the mSpace system [68] in the multimedia domain, BrowseRDF [60] in the crime domain, /facet [43] and Ontogator [52] in the art domain, or more recently, ReVeaLD [48] in the biomedical domain, and Hippalus [71] in the zoology domain. Such works typically have dealt with smaller-scale and/or homogeneous graphs with few classes and properties, focusing on usability and expressivity rather than issues of scale or performance.

However, with the growth of large-scale multi-domain knowledge graphs like DBpedia, Freebase or Wikidata, a number of faceted browsers have been proposed that support thousands of classes and properties and upwards of a hundred million edges, as needed for such datasets. Among these systems, we can mention Neofonie [40], Rhizomer [19], SemFacet [10], Semplore [77] and Sparklis [33] for exploring DBpedia; Broccoli [14] and Parallax [46] for exploring Freebase; and GraFa for exploring Wikidata [54]. Of these systems, many do not present runtime performance evaluation [19, 40, 46, 76], delegate query processing to a general-purpose query engine [19, 33, 41, 46], apply a manual selection of useful facets or a subset of data [10, 40], and/or otherwise rely on a materialization approach to cache metadata (such as counts) [14, 19, 54]. Compared to such works, we focus on scalability and performance; more concretely, we propose a novel query engine specifically optimized for the types of online aggregation queries needed by such systems.

*Graph Profiling:* While faceted browsing aims to allow users to express and answer specific questions in an intuitive manner, other works have focused on the problem of summarizing the content of a large knowledge graph: to provide users insights as to what the graph does or does not contain, what are the relationships between entities, what are the most common types, and so forth [31].

One approach to provide users with an overview of a knowledge graph is to compute a *graph summary* or *quotient graph* [24], which groups nodes into super-nodes, between which the most important relations are then summarized. The conceptual summarization can be conducted by a number of techniques, including, for example, variations on the idea of bisimulations [21, 27, 62, 67], formal concept analysis [7, 29, 37, 50, 66], semantic types [22, 30, 34, 49], etc. Other such works rather focus on generating statistical summaries of large graphs, in terms of the most popular classes, properties, etc., generating bar charts and other (possibly interactive) visualizations [4, 12, 15, 35, 53, 63]. While such works tackle a variety of different use-cases using a diverse

collection of techniques, all are founded on aggregation operations applied to nodes and relationships – either offline or using general-purpose query engines – generating high-level descriptions of the graph. The aggregation algorithms we propose are online and more efficient than general-purpose query algorithms, and could be readily adapted to the various use-cases explored in the aforementioned literature.

## Query Engines

We provide an overview of approaches for querying knowledge graphs that most closely relate to this work.

*SPARQL Engines:* A variety of query languages have been proposed for graphs [9]. Among these, SPARQL [3] is the standard language for querying RDF graphs, and is used, for example, by public query services over the DBpedia, Linked-GeoData, and Wikidata knowledge graphs. While several query engines support SPARQL (e.g., [16, 55, 70]), in this paper we take Virtuoso [2] as a baseline query engine given its competitiveness in a number of benchmarks [8, 20]. Virtuoso maintains clustered indexes in various (redundant) orders needed to support efficient lookups on RDF graphs; these clustered indexes support both row-wise and column-wise operations where, for example, a row-wise index can be used to find a particular row from which to start reading values from a given column. To optimize for aggregate-style queries, Virtuoso applies vectorized execution on a column represented as a compressed vector of values.

*Worst-Case-Optimal Joins:* A number of worst-case optimal join algorithms have been developed in recent years [5, 6, 47, 56, 73]. These algorithms evaluate join queries with a runtime that meets the Atserias–Grohe–Marx (AGM) bound [11], which, given a join query, provides a worst-case tight bound for the size of the output. It was shown that these algorithms are not only theoretically better than traditional approaches, they are also empirically superior on graph query patterns joining relations with low dimension [5, 47, 58]. In this paper, we will adopt Cached Trie Join – a state-of-the-art worst-case optimal join algorithm – and contrast it with Virtuoso for answering aggregate queries generated by our exploration system; we subsequently combine this algorithm with online aggregation techniques to trade precision for performance.

*Online Aggregation:* Algorithms for online aggregation provide approximate results that converge over time to the exact aggregate queries. Since the concept was coined by Hellerstein et al. [42] this class of algorithms grew to support additional operators and better statistical guarantees [38], as well as distributed and parallel support [61, 64, 65]. While the solution was originally for a single table, Haas et al. [39] developed Ripple Join, an online aggregation algorithm that supports joins. More recently, Li et al. [51] have introduced

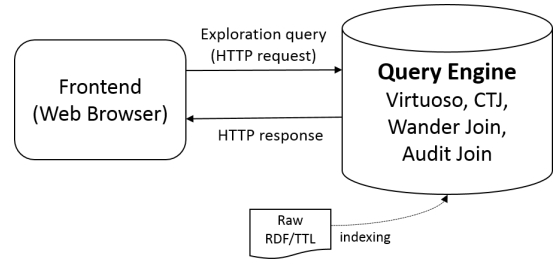


Figure 1: General system architecture

the Wander Join algorithm for online aggregation over join results. Wander Join uses random walks over the indexes of the joined tables to sample results. Paths that cover all joins are considered valid sampled results, while partial paths constitute rejected samples; online aggregation can then be applied on these samples as they are collected. Wander Join has also been used as an unbiased sampling method for approximate query answering [36] and join-size estimation [25]. We describe Wander Join in more detail in Section 5.

In this paper, we use Cached Trie Join to reduce the rejection rate of Wander Join for selective patterns; we further prove that this strategy provides an unbiased estimator of counts with and without a distinct operator, where, to the best of our knowledge, no existing online aggregation algorithm offers unbiased estimators in the distinct case.

## 3 SYSTEM OVERVIEW

The focus of this work is on our formal exploration model, and its efficient realization as an interactive system. To give the intuition behind our approach, we begin with a high-level description of our implemented system;<sup>5</sup> in the next sections, we delve into the formal model and algorithms. Our system offers online exploration of large-scale knowledge graphs and is implemented as a Web application that communicates with a specialized query engine, as illustrated in Figure 1.

Currently our system supports exploration of an RDF graph: a set of RDF triples of the form  $(s, p, o)$  where  $s$  is called the *subject*,  $p$  is called the *predicate*, and  $o$  is called the *object*. An RDF graph can thus be considered as a directed edge-labeled graph in which each triple encodes an edge  $s \xrightarrow{p} o$ . Nodes in this RDF graph may be instances of *classes* (e.g. Person, Movie, etc.) where these classes may be further organized into a *subclass hierarchy* (e.g., defining Movie to be a subclass of Work). We further refer to terms used in the predicate position of a triple (e.g., director) as *properties*. We will provide more detail on RDF graphs in Section 5.

During exploration of the graph, the Web application generates queries that are sent via HTTP to the backend. In this

<sup>5</sup>The system has been demonstrated and described in a demo paper [1].

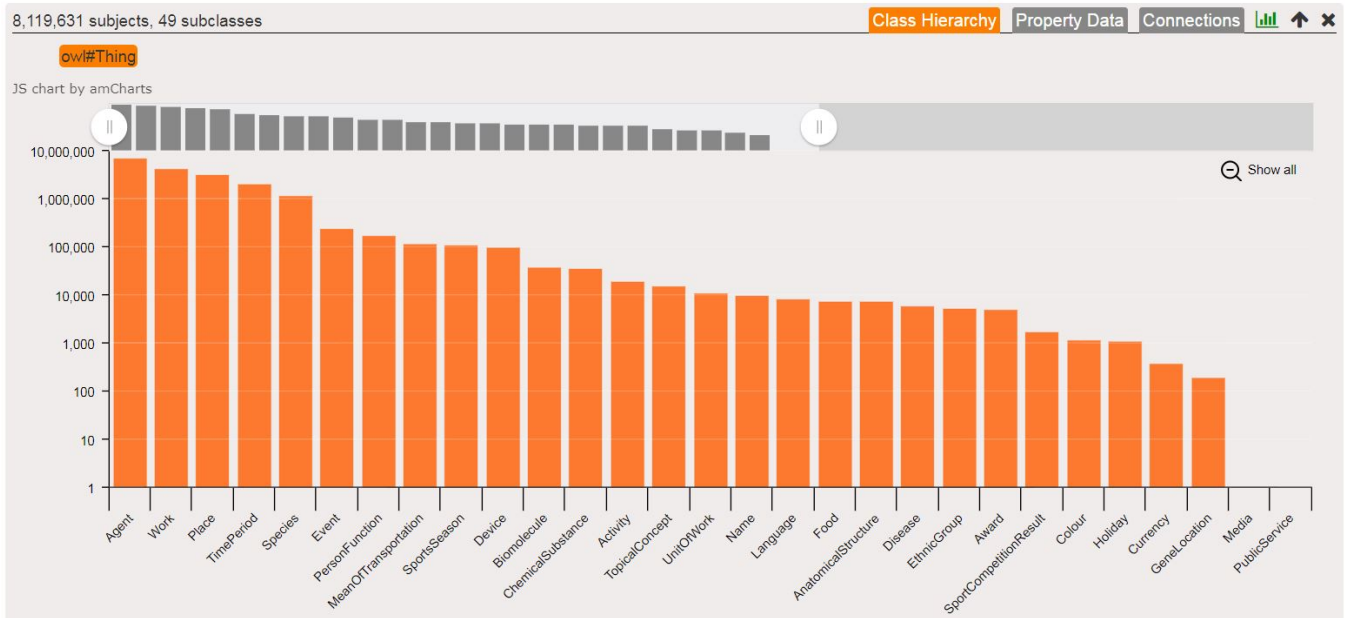


Figure 2: Initial chart in the exploration pane over DBpedia.

backend, the system can use any query engine that supports aggregate queries over graph patterns (more specifically, count and count–distinct operations over groupings of results for join queries). Our system currently implements four alternative query engines, which we describe in more detail in Section 5: Virtuoso [2], Cache Trie Join (CTJ) [47], Wander Join [51], and Audit Join—our bespoke algorithm for online aggregation that we describe in Section 5.

The user experience is visual, and no SPARQL knowledge is required from the user. In principle, the user should have only a basic understanding of what classes and properties are. Next, we provide an overview of the user interface, and illustrate the concept and functionality of our system through an example exploration over the DBpedia dataset [17].

### 3.1 User Interface

The basic UI component is a *tabbed pane*, as illustrated in Figure 2. Each tab in the pane presents a specific *bar chart*, which is the result of an *expansion* applied on a bar of a previous pane. (We present our formal exploration model in Section 4.) The tab in Figure 2 shows the initial bar chart for DBpedia. The bar chart visualizes the distribution of all DBpedia subjects (instances of class owl:Thing) into subclasses. Each bar matches a specific subclass, with a height proportional to its number of instances. The bars are sorted by decreasing height. Hovering over a bar opens a pop-up box with basic information such as the number of instances, and the number of direct and indirect subclasses. To support

visualization of large charts with many classes or properties, a widget allows to control the visible part of the chart.

The user can then navigate down the class hierarchy in order to focus the exploration on a set of instances in a class of interest. Class navigation is done by clicking a bar, which opens a new pane under the current one. (In cases where top-down class navigation is less intuitive, our system offers an autocomplete search box for class types, based on a list that is populated by collecting all subjects of type owl:Class or rdfs:Class. Selecting a class in this way immediately opens the associated pane without the need to drill down.)

A second tab in the pane shows a *property chart*—the result of what we call a *property expansion*, as illustrated in Figure 3. Here, each bar represents a specific property and the count represents distinct elements of the current focus set with some value for that property. By default, properties that emanate from the focus set (*outgoing properties*) are shown, but the user may switch to displaying the *incoming properties* for the current focus set. Bars are then sorted by *coverage*—the percentage of focus elements that have the property as outgoing or incoming, respectively. The number of properties may be very large, and therefore, our system supports filtering out properties with a coverage lower than a threshold adjustable by the user. For example, in Figure 3, only 57 properties out of 722 possible properties are shown.

Getting general statistics about the dataset and its classes is essential, yet a user may be interested in looking into the specific instances of the dataset as well. For that, a *data table* that appears below the property chart shows the values of

selected properties (bars) in the chart. The SPARQL query used to generate the data table may be retrieved by the user for downstream consumption. *Data filters* attached to table columns may restrict the displayed data.

### 3.2 Illustrating Example

To illustrate the system, consider the following scenario. Suppose that the user is interested in philosophers, and in particular, they wish to learn about people who have influenced philosophers. The exploration starts by navigating to the class *Philosopher*. It is done by opening three subsequent panes: *Agent*  $\rightarrow$  *Person*  $\rightarrow$  *Philosopher*. Then, switching to the property chart reveals the most significant outgoing properties that philosophers have in DBpedia, one of them being *influencedBy*. Selecting this property and applying an *object expansion* opens a new pane, showing the different class types connected to philosophers via the *influencedBy* property. Clicking the *Person* type reveals the pane shown in Figure 3, with instances of type *Person* connected to philosophers (via that property). This allows the user to further explore *only* people who have influenced philosophers and not the entire *Person* set. Furthermore, a *filter* allows to restrict the bar chart to the people born in *Austria* (who have influenced philosophers), as shown in the figure.

## 4 EXPLORATION MODEL

In this section, we describe our formal framework for exploring knowledge graphs. We begin with an intuitive overview.

### 4.1 General Idea

The formal model underlying our exploration language iteratively applies the basic principle for effective data visualization by Shneiderman [69] mentioned previously: “Overview first, zoom and filter, then details-on-demand.” Specifically, our formal model is based on bar charts over focus sets of nodes (URIs) that are constructed incrementally by the user. The model is based on the following components.

- A *bar chart* consists of a set of *bars*, each representing a portion of the focus set. Figure 2, for example, depicts a bar chart in our implemented system.
- The user selects a bar from the bar chart, and applies an *expansion operation* that transforms a bar into a new bar chart; the portion of the selected bar becomes the focus set of the new bar chart.
- Another operation is *filtering* that can be applied to restrict the bar chart (and each bar within) according to a Boolean criterion over the focus set. Hence, this operation transforms one bar chart into another one.

The user can then continue the exploration of the new bar chart, and hence, construct focus sets of arbitrary depths.

In what follows, we give a formal definition of the data and exploration model.

### 4.2 Formal Framework

We now present the formal framework.

**RDF graphs.** We adopt a standard model of RDF data (omitting blank nodes for brevity). Specifically, we assume collections  $U$  of *Unique Resource Identifiers* (URIs) and  $L$  of *literals*. An *RDF triple*, is an element of  $U \times U \times (U \cup L)$ . An *RDF graph* is a finite collection  $G$  of RDF triples. In the remainder of this section, we assume a fixed RDF graph  $G$ . A URI  $u$  is said to be *of class*  $c$  if  $G$  contains the triple  $(u, \text{rdf:type}, c)$ . One could also define membership in a class by joining the *rdf:type* value with the *transitive/reflexive closure* on subclasses; the choice between the two is orthogonal to our model.

**Bar charts.** We model the visual exploration of the RDF graph  $G$  by means of bar charts that are constructed in an iterative, interactive manner. We have three kinds of bars:

- A *class bar* represents URIs with a common class (e.g., the class *Person*).
- An *outgoing-property bar*, or *out-property bar* for short, represents URIs that are the subject (source) of a common associated outgoing property (e.g., subjects of locatedIn triples).
- Analogously, an *incoming-property bar*, or *in-property bar* for short, represents URIs that are the object (target) of a common associated incoming property (e.g., objects of locatedIn triples).

For a bar  $B$ , we denote by  $U(B)$  the set of URIs represented by  $B$ . The *category* of  $B$  is the corresponding class or property, depending on the kind of  $B$ . A *bar chart* (or simply “*chart*” in what follows) is a mapping from categories to bars.

**Bar expansion.** A *bar expansion* is a function  $E$  that transforms a given bar  $B$  into a chart  $E(B)$ . We define specific bar expansions  $E$  that are also implemented in our system. As a consequence, we arrive at a transition system between chart types, as depicted in Figure 4.

Subclass expansion: This expansion is allowed only on class bars  $B$ ; in this case, the category  $c$  of  $B$  is a class. The categories of the chart  $E(B)$  are all the *subclasses* of  $c$ ; that is, the URIs  $c'$  such that  $G$  contains the triple  $(c', \text{rdfs:subClassOf}, c)$ . The bar  $B_{c'}$  that  $E(B)$  maps to  $c'$  is a class bar with the category  $c'$ , and the set  $U(B_{c'})$  consists of all the URIs  $u \in U(B)$  such that  $u$  is of the class  $c'$ .

Out-property expansion: This expansion is only allowed on a class bar  $B$ . The categories of the chart  $E(B)$  are the outgoing properties of the URIs of  $B$ ; that is, the URIs  $p$  such that  $G$  contains  $(s, p, o)$  for some  $o$  and  $s \in U(B)$ . The bar  $B_p$  that  $E(B)$  maps to  $p$  is an out-property bar with category  $p$ .

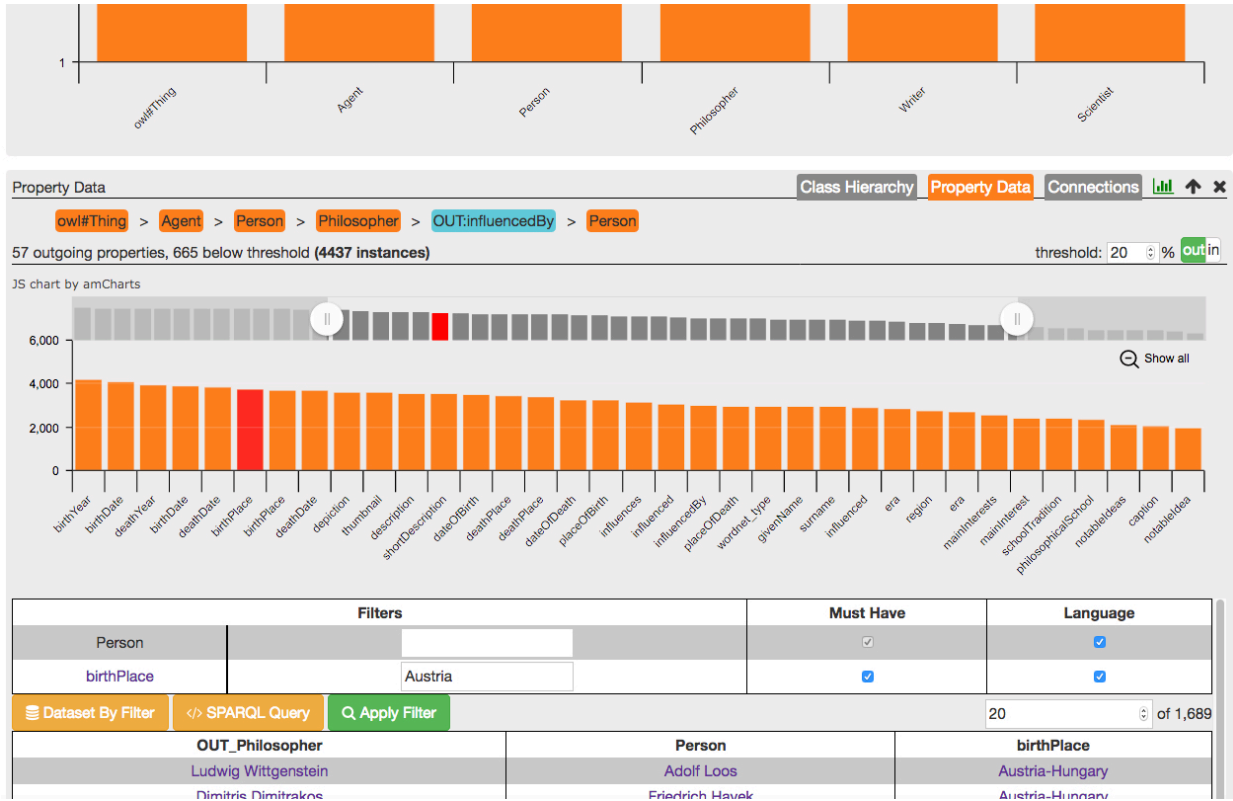


Figure 3: Two exploration panes over DBpedia (upper is partially visible). Lower pane shows property data about *persons who have influenced philosophers*.

The set  $U(B_p)$  consists of all URIs  $s \in U(B)$  with the property  $p$ ; that is, all  $s \in U(B)$  such that  $(s, p, o) \in G$  for some  $o$ .

**In-property expansion:** This expansion is analogous to the out-property expansion, except that the bar  $B_p$  mapped to  $p$  by  $E(B)$  is an *in-property* bar with the category  $p$ , and  $U(B_p)$  consists of all URIs  $o \in U(B)$  that have the incoming property  $p$ ; that is, all  $o \in U(B)$  such that  $(s, p, o) \in G$  for some  $s$ .

**Object expansion:** This expansion is enabled only for out-property bars  $B$ ; recall that, in this case, the category of  $B$  is a property  $p$ . The categories of the chart  $E(B)$  are the classes  $c$  of the *objects* that are connected to the URIs in  $U(B)$  through

the property  $p$ ; that is, the classes  $c$  such that for some triple  $(s, p, o) \in G$  it is the case that  $s \in U(B)$  and  $o$  is of class  $c$ . The bar  $B_c$  that  $E(B)$  maps to  $c$  is a class bar with the category  $c$ , and  $U(B_c)$  consists of the  $p$ -targets of type  $c$ ; that is, all URIs  $o$  of class  $c$  such that  $(s, p, o) \in G$  for some  $s \in U(B)$ .

**Subject expansion:** This expansion is analogous to the object expansion, but considers the subjects of incoming properties rather than the objects of outgoing properties. Specifically, this expansion is enabled only for in-property bars  $B$ , where the category of  $B$  is a property  $p$ . The categories of  $E(B)$  are the classes  $c$  of the *subjects* that are connected to the URIs in  $U(B)$  through the property  $p$ ; that is, the classes  $c$  such that for some triple  $(s, p, o) \in G$  it is the case that  $o \in U(B)$  and  $s$  is of class  $c$ . The bar  $B_c$  that  $E(B)$  maps to  $c$  is a class bar with the category  $c$ , and  $U(B_c)$  consists of the  $p$ -sources of type  $c$ ; that is, all URIs  $s$  of class  $c$  such that  $(s, p, o) \in G$  for some  $o \in U(B)$ .

**Exploration.** Our model enables the exploration of  $G$  by allowing the user to construct a list of bar charts in sequence, with each successive chart exploring a bar of the previous chart. The exploration begins with a predefined *initial chart*

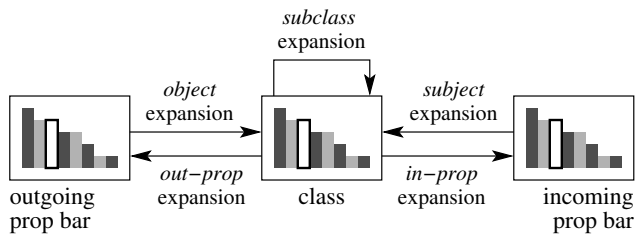


Figure 4: State transitions in the exploration model

that we denote by  $\mathbf{B}_0$ . In our implementation, this bar has the form  $E(B)$  where  $E$  is the subclass expansion and  $B$  is a bar that consists of all URIs of a predefined class; a sensible choice for this class is a general type such as owl:Thing. By *exploration* we formally refer to a sequence of the form

$$\mathbf{B}_0 \mapsto (c_1, E_1) \mapsto \mathbf{B}_1, (c_2, E_2) \mapsto \mathbf{B}_2, \dots, (c_m, E_m) \mapsto \mathbf{B}_m$$

where each chart  $\mathbf{B}_i$  is obtained by selecting the bar  $B$  of category  $c_i$  from the chart  $\mathbf{B}_{i-1}$  and applying to  $B$  the expansion  $E_i$  (assuming  $E_i$  is allowed on  $B$ ).

**Filtering.** In addition to the collection of expansion operations, the model and implemented system also allow for *filtering* conditions, such as “restrict to all URIs  $s$  who were born in Africa”; that is, for some  $c$  it is the case that  $(s, \text{bornIn}, c) \in G$  and  $(c, \text{name}, \text{'Africa'}) \in G$ . Formally, a condition is abstracted simply as a subset  $F$  of  $U$ ; when applying  $F$  to a chart  $\mathbf{B}$ , the resulting chart is obtained from  $\mathbf{B}$  by restricting  $U(B)$  to  $F \cap U(B)$  for every bar  $B$ .

*Example 4.1.* For illustration, we consider another DBpedia scenario, now expressed in the terminology of the formal exploration model. Suppose that the user is interested in understanding what information DBpedia has on cities where scientists were born. The initial bar chart shown (Figure 2) is the result of a subclass expansion applied to the bar  $B$  that corresponds to (i.e.,  $U(B)$  consists of) all URIs of type owl:Thing. A total of 49 top-level classes (bars) are shown, where the user may observe that the most popular classes are Agent and Work. The user then applies a subclass expansion on the Agent bar to build a bar chart over the agents. Additional subclass expansions are then applied to focus on the Scientist nodes (through class Person). Next, an out-property expansion is applied to get the distribution of outgoing properties of scientists, and from there the user selects the birthPlace bar. An object expansion over this bar results in the bar chart over the birth places of scientists, and from there the user selects the City bar.  $\square$

## 5 QUERY ENGINE AND ALGORITHMS

To feature interactive exploration, the underlying query engine of the system should answer multiway join queries in less than a second. However, in initial experiments with the Virtuoso system, such queries would sometimes take minutes to complete. Algorithms that implement worst-case-optimal joins have recently been shown to be capable of orders-of-magnitude speedup compared to traditional join approaches [57, 59], and hence, offer a promising alternative. Still, in experiments with Cached Trie Join [47] – a state-of-the-art representative of these join algorithms – queries that require large join results on multi-domain knowledge graphs (e.g., DBpedia) may still take tens of seconds to run.

With the goal of reaching acceptable performance, we turn to *online aggregation*, relaxing the expectation of exact counts to instead aim for a fast but approximate initial response whose error reduces over time [42]. Such a compromise is well justified in the context of this work, since queries are used for rendering bar charts that can suffer loss of precision with limited impact on the user experience. Along these lines, we investigate use of Wander Join [51], which is designed for aggregate queries over the grouped results of join queries; this algorithm has been empirically demonstrated to offer much better convergence compared to traditional online aggregation approaches in experiments over TPC-H [51]. However Wander Join has two limitations in our specific use-case: (1) rejected paths slow convergence of the estimations, and (2) it does not support (i.e., provide an unbiased estimator) for the count-*distinct* operator.

We thus propose a novel online-aggregation algorithm, Audit Join, which addresses these limitations of Wander Join. First, in cases where a high number of rejected paths are deemed likely to occur, Audit Join defers to partial exact computations using Cached Trie Join. Second, Audit Join incorporates a novel estimator for counts under the distinct operator that we prove to be unbiased.

This section now discusses the various algorithms we employ to improve query performance in our interactive exploration setting, starting with preliminaries on query translation, then discussing Cached Trie Join and Wander Join, before detailing our Audit Join proposal.

### 5.1 Query Translation and Structure

Section 4 defined our exploration model. The five operations of subclass, in-property, out-property, object and subject expansions are translated to SPARQL queries via our query engine. These SPARQL queries produce the information required to generate the next bar chart by first executing a multiway join that encodes the expansions thus far, then a grouping on the URIs of the next chart, and finally a distinct count on the focus set of the next chart. Due to the structure of exploration steps, cyclic queries cannot occur.

The general form of these SPARQL queries is illustrated by the query template in Figure 5. Here, each pattern of the form  $a_i b_i c_i$  refers to a *triple pattern*, where each term  $a_i$ ,  $b_i$  and  $c_i$  (where  $1 \leq i \leq n$ ) is either a variable (e.g., ?s) or a constant (e.g., <Person>). A variable may appear in at most two triple patterns. Finally,  $\alpha$  denotes a variable that will be assigned the URIs of the next bar chart (either some  $b_i$ , or some  $c_i$  where  $b_i = \text{rdf:type}$ ), while  $\beta$  returns the focus set of the next bar chart (either some  $a_i$  or  $c_i$ ). As an example, the exploration *birthplaces of persons* is translated to the SPARQL query shown in Figure 6.

```

SELECT  $\alpha$  COUNT(DISTINCT  $\beta$ ) WHERE {
   $a_1$   $b_1$   $c_1$  .
  ...
   $a_n$   $b_n$   $c_n$  .
} GROUP BY  $\alpha$ 

```

**Figure 5: The general form of an exploration query**

REMARK. *In practice, triple patterns with the “rdf:type” property are joined with the reflexive/transitive closure of subclasses. For example, in the pattern “?sc rdf:type <Person>” of Figure 6, ?sc will also be mapped to instances of (possibly indirect) subclasses of <Person>. We materialize this subclass closure and view it as a raw relation; instances, on the other hand, are typed per the original data and joined with the subclass closure at runtime. For simplicity, we leave the subclass closure implicit in the presentation of the queries since, as previously mentioned, it is orthogonal to the model.* □

In the remainder of this section, we denote by  $G_i$  the subset of  $G$  that consists of all the triples of the knowledge graph  $G$  that match the triple pattern  $(a_i, b_i, c_i)$ , where a triple  $(a, b, c)$  matches  $(a_i, b_i, c_i)$  if the two agree on the constants (that is, if  $a_i$  is a constant then  $a = a_i$ , and so on).

## 5.2 Aggregation via Cached Trie Join

The exact evaluation we incorporate in our approach is based on the *Cached Trie Join* algorithm (CTJ) [47]. This algorithm incorporates caching of intermediate join results on top of the *LeapFrog Trie Join* algorithm (LFTJ) [73]—a backtracking join algorithm that traverses over trie indexes. In our context, we maintain six trie indexes over  $G$ , each corresponding to an ordering of the three attributes ( $s$ ,  $p$  and  $o$ ). The trie index has a root, and under the root a layer with the values of the first attribute, and then a layer with the values of the second attribute, and then the third attribute. Each triple  $(s, p, o)$  corresponds to a unique root-to-leaf path of the trie. For example, if the order is  $(p, o, s)$ , then the first layer corresponds to the predicates, the second to the objects, and the third to the subjects; in this case, a path  $\text{root} \rightarrow b \rightarrow c \rightarrow a$  represents the triple  $(a, b, c)$  of  $G$ . In our implementation, B-tree

```

SELECT ?c COUNT(DISTINCT ?o) WHERE {
  ?s <birthPlace> ?o.
  ?s rdf:type ?sc.
  ?sc rdf:type <Person>.
  ?o rdf:type ?c.
} GROUP BY ?c

```

**Figure 6: An instance of an exploration query**

like indexes are used, similar to the indexes commonly used in SPARQL (and other) query engines.

LFTJ assumes a predetermined order over the variables, say  $x_1, \dots, x_m$ . We access the tuples of  $G_i$  using a trie  $T_i$  with an order that is consistent with the predetermined order. For example, if the triple  $a_i b_i c_i$  is ?q <birthPlace> ?r and ?r precedes ?q in the predefined order, then  $T_i$  will be the trie for  $(o, s, p)$ ,  $(o, p, s)$ , or  $(p, o, s)$ . LFTJ uses a backtracking algorithm that walks over the  $T_i$  and looks for assignments for  $x_1, \dots, x_m$ . It starts by finding the first matching value  $v_1$  for  $x_1$ . Then, the tries  $T_i$  that contain  $x_1$  restrict their search to the subtree under  $x_1 = v_1$ . Next, it looks for the first match  $v_2$  of the next variable  $x_2$ , and all relevant tries restrict to the subtree under  $x_2 = v_2$ . The algorithm continues to remaining variables, until a match is found for all variables, or it cannot find a matching value for the next variable. Once a match is found, or the algorithm gets stuck, it backtracks to the next value of the previous scanned  $x_i$ . Grouping and counting are applied in the straightforward manner.

While LFTJ guarantees worst-case optimality, it frequently re-computes the same intermediate joins, since it does not materialize any of the intermediate results [47]. To effectively reuse the partial answers, CTJ augments LFTJ with a cache structure guided by a tree decomposition of the query, guaranteeing the correctness of the algorithm. In the use case of this paper, the tree decomposition is easily determined by the path formed by the query. CTJ uses different caching schemes to cache partial count results that are later reused. Empirically, CTJ can achieve orders of magnitude speedup over LFTJ and other known join algorithms for graph queries on relations with a low dimension [47].

## 5.3 Wander Join

Wander Join is an online aggregation algorithm that is designed for aggregates over joins [57, 59]. Since Wander Join does not support the distinct operator, we ignore the operator in this section. For presentation sake, we begin by also ignoring the grouping operator, and assume that we only need to count the number of matches for the variables. We discuss grouping later in the section.

Given the query of Figure 5, Wander Join samples query answers via independent random walks over the  $G_i$ , in contrast to the full pre-order traversal of CTJ. It estimates the count by adopting the Horvitz-Thompson estimator [45], where each random walk  $\gamma$  produces an estimator  $C_{\text{wj}}(\gamma)$  that we describe next, and the final estimator is simply the average of the  $C_{\text{wj}}(\gamma)$  over all random walks  $\gamma$ . The walk  $\gamma$  is constructed as follows. We first select a random tuple  $t_1$  uniformly from  $G_1$ . Next, select a tuple  $t_2$  that is consistent with  $t_1$ ; that is,  $t_1$  and  $t_2$  agree on the common attributes; the choice is again uniform among all consistent  $t_i$ . We continue



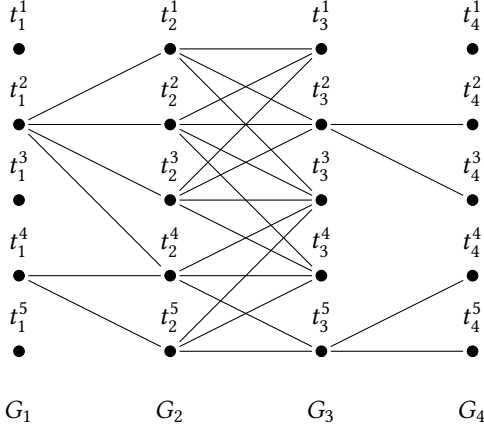


Figure 7: A join graph

in this way, where in the  $i^{\text{th}}$  step we select a random tuple  $t_i$  from  $G_i$  such that  $t_i$  is consistent with  $t_{i-1}$ . If, at any point, no matching  $t_i$  exists, then the random walk  $\gamma$  terminates and  $C_{\text{wj}}(\gamma) = 0$ . Otherwise, denote by  $d_i$  the number of possible ways of selecting  $t_i$ , for  $i = 1, \dots, n$ . Note that the probability of  $\gamma$  is  $\prod_{i=1}^n 1/d_i$ . The estimator  $C_{\text{wj}}(\gamma)$  is defined by

$$C_{\text{wj}}(\gamma) := \prod_{i=1}^n d_i = \frac{1}{\Pr(\gamma)}.$$

The estimator  $C_{\text{wj}}(\gamma)$  is unbiased; consequently, the final estimator (i.e., the average) is also unbiased. To see why  $C_{\text{wj}}$  is unbiased, denote by  $\Gamma$  the set of all successful (full) paths from  $G_1$  to  $G_n$ . Then the sought count is  $|\Gamma|$ . Indeed,

$$\mathbb{E}[C_{\text{wj}}] = \sum_{\gamma \in \Gamma} \Pr(\gamma) \cdot C_{\text{wj}}(\gamma) = \sum_{\gamma \in \Gamma} \frac{\Pr(\gamma)}{\Pr(\gamma)} = |\Gamma|.$$

*Example 5.1.* We demonstrate Wander Join using the example join graph depicted in Figure 7. There, each column in the figure is a graph  $G_i$ , and each node  $t_i^j$  is a tuple of  $G_i$ . An edge exists between two tuples if they agree on their join attributes. The random walk is from left to right. Choosing the random path  $\gamma_1 = (t_1^2, t_2^2, t_3^2, t_4^2)$  yields the estimate  $C_{\text{wj}}(\gamma_1) = 5 \cdot 4 \cdot 4 \cdot 2 = 160$ . For  $\gamma_2 = (t_1^4, t_2^5, t_3^5, t_4^5)$  we will get  $C_{\text{wj}}(\gamma_2) = 5 \cdot 2 \cdot 3 \cdot 2 = 60$ . Finally, partial paths, such as  $(t_1^2, t_2^2, t_3^3)$ , will yield the estimate zero. The final estimator is the average over all estimates.  $\square$

Wander Join adapts to *grouping* in a manner similar to that of Ripple Join [39]: maintaining a separate estimator for each group, and using the random  $\gamma$  to update only the separator of the group to which  $\gamma$  belongs.

## 5.4 Audit Join

For presentation sake, we first describe Audit Join while ignoring the distinct operator. Again, we also ignore grouping, since Audit Join is adapted to grouping similarly to Wander Join and Ripple Join. Hence, our goal is again to estimate  $|\Gamma|$ , where  $\Gamma$  is the set of all full random walks  $\gamma$  from  $G_1$  to  $G_n$ .

The basic idea is as follows. For a prefix  $\delta = (t_1, \dots, t_\ell)$  of a random walk, denote by  $\Gamma_\delta$  the set of full paths  $\gamma$  with the prefix  $\delta$ . At each step of the random walk, we make a rough estimation of the complexity of computing the precise  $|\Gamma_\delta|$ ; we describe this estimation in Section 5.4.1. If the estimate is low, we actually compute  $|\Gamma_\delta|$  using CTJ (as described in Section 5.2), and then our estimate is

$$C_{\text{aj}}(\delta) := |\Gamma_\delta| \times \prod_{i=1}^{\ell} d_i = \frac{|\Gamma_\delta|}{\Pr(\delta)}.$$

Otherwise, we proceed exactly as Wander Join. In particular, if we cannot continue in the random walk, or reach a full path, then we use  $C_{\text{aj}}(\delta) = C_{\text{wj}}(\delta)$ .

*Example 5.2.* We illustrate Audit Join (without distinct) by continuing our example over Figure 7. Suppose that after the random walk  $\delta = (t_1^2, t_2^2)$ , we choose to run an exact evaluation. Then  $|\Gamma_\delta| = 2$ , since there are two full paths (ending at  $t_4^2$  and  $t_4^3$ ) that begin with  $\delta$ . Then the estimation is  $C_{\text{aj}}(\delta) = |\Gamma_\delta|/\Pr(\delta) = 2 \cdot (5 \cdot 4) = 40$ .  $\square$

In the following proposition, we show that  $C_{\text{aj}}$  is unbiased by straightforwardly adapting the argument for Wander Join.

**PROPOSITION 5.3.**  $C_{\text{aj}}$  is an unbiased estimator of  $|\Gamma|$ .

**PROOF.** Let  $\Delta$  be the set of all paths  $\delta$  where Audit Join decides to terminate the path and produce an estimate. This can be because  $\delta$  is a full path, because it cannot proceed, or because we decide to compute the exact  $|\Gamma_\delta|$ . The reader can verify that, no matter which of the three is the case, Audit Join produces the same estimator, namely  $|\Gamma_\delta|/\Pr(\delta)$ . In particular,  $|\Gamma_\delta| = 1$  in the first case and  $|\Gamma_\delta| = 0$  in the second. We have the following.

$$\mathbb{E}[C_{\text{aj}}] = \sum_{\delta \in \Delta} \Pr(\delta) \cdot \frac{|\Gamma_\delta|}{\Pr(\delta)} = \sum_{\delta \in \Delta} |\Gamma_\delta| = |\Gamma|$$

Therefore,  $C_{\text{aj}}$  is unbiased, as claimed.  $\square$

Note that Audit Join automatically leverages the caching of CTJ, potentially avoiding re-computation when building the same prefix  $\delta$  in later random walks.

We now extend our estimator to support the distinct operator. Recall the query of Figure 5. Our goal is to count the distinct values taken by  $\beta$ . For a full path  $\gamma$ , we denote by  $\beta(\gamma)$  the value to which  $\gamma$  assigns  $\beta$ . Let  $V = \{\beta(\gamma) \mid \gamma \in \Gamma\}$ . Our goal is to estimate  $|V|$ . For  $b \in V$ , we denote by  $\Pr(b)$  the probability that the random walk reaches a full path  $\gamma$  with

$\beta(\gamma) = b$ ; that is,  $\Pr(b)$  is the sum of the probabilities of all  $\gamma \in \Gamma$  that assign  $b$  to  $\beta$ . Similarly, we denote by  $\Pr(\delta, b)$  the probability that the random walk starts with  $\delta$  and reaches a full path  $\gamma$  with  $\beta(\gamma) = b$ ; that is,  $\Pr(\delta, b)$  is the sum of the probabilities of all  $\gamma \in \Gamma$  such that  $\alpha$  is a prefix of  $\gamma$  and  $\gamma$  assigns  $b$  to  $\beta$ . We then combine these probabilities into the following estimator for distinct.

$$C_{aj}^d(\delta) := \sum_{b \in V} \frac{\Pr(\delta, b)}{\Pr(\delta) \cdot \Pr(b)} \quad (1)$$

*Example 5.4.* To demonstrate Audit Join with count distinct, we again use our running example over Figure 7. For this example, suppose that  $\beta$  occurs in  $G_3$ , and moreover, that each tuple  $t_3^i$  holds a unique value for  $\beta$  (while many join tuples may include  $t_3$ ). Suppose that the random walk produces  $\delta = (t_1^2, t_2^2)$ , and that Audit Join decides to run an exact evaluation at this point. There are two full paths that extend  $\delta$ , both through  $(t_2^3)$ . We denote by  $b$  the value of  $\beta$  for  $(t_2^3)$ . From the previous example we get that  $\Pr(\delta) = \frac{1}{20}$ . There are three paths leading to  $t_2^3$ , and by summing their probabilities we get  $\Pr(b) = \frac{1}{5 \cdot 4 \cdot 3} + \frac{2}{5 \cdot 4 \cdot 4} = \frac{1}{24}$ . The last probability of our estimator is

$$\Pr(b, \delta) = \Pr(b \mid \delta) \cdot \Pr(\delta) = \frac{1}{4} \cdot \frac{1}{20} = \frac{1}{80}.$$

Hence, our estimator yields the following.

$$C_{aj}^d(\delta) = \frac{\Pr(\delta, b)}{\Pr(b) \cdot \Pr(\delta)} = \frac{20 * 24}{80}$$

Hence, the estimate  $C_{aj}^d(\delta)$  is 6.  $\square$

In our implementation, the probability  $\Pr(b)$  is computed by using CTJ to materialize all paths leading to  $b$  and summing up their probabilities. Clearly, this can be an expensive join query, and our cost estimation (described in Section 5.4.1) guards us from costly cases. Nevertheless, as we show in Section 6, it turns out that in our use case this computation is very often tractable, hence the considerable benefit of Audit Join. Next, we show that the estimator is unbiased.

**PROPOSITION 5.5.**  $C_{aj}^d$  is an unbiased estimator of  $|V|$ .

**PROOF.** Following a similar reasoning as in the proof of Proposition 5.3, we can treat all cases of the estimator in a uniform way, that is, according to Equation (1). In the following analysis, we identify value  $b \in V$  with the event that the random walk is complete and, moreover, assigns  $b$

---

AuditJoin( $G_1, \dots, G_n, \alpha, \beta$ )

---

```

1:  $N := 0$ 
2:  $A :=$  the set of possible assignments for  $\alpha$ 
3:  $B :=$  the set of possible assignments for  $\beta$ 
4: repeat
5:    $F_1 := G_1$ 
6:    $\delta := \epsilon$ 
7:   for  $i = 1, \dots, n$  do
8:      $N := N + 1$ 
9:     select  $t \in F_i$  randomly and uniformly
10:     $\delta := (\delta, t)$ 
11:    if  $i = n$  or tipping point is reached then
12:      for all  $a \in A$  do
13:         $C_a := C_a + \sum_{b \in B} \frac{\Pr(a, b, \delta)}{\Pr(a, b) \cdot \Pr(\delta)}$ 
14:      end for
15:      continue ▷ Go to line 5
16:    end if
17:     $F_{i+1} := G_{i+1} \times t$ 
18:    if  $F_{i+1} = \emptyset$  then
19:      continue ▷ Go to line 5
20:    end if
21:  end for
22: until time limit is reached
23: for all  $a \in A$  do
24:   estimate count-distinct for  $a$  as  $C_a/N$ 
25: end for

```

---

**Figure 8: Audit Join pseudo code**

to  $\beta$ . Hence, we have the following.

$$\begin{aligned} \mathbb{E}[C_{aj}^d] &= \sum_{\delta \in \Delta} \Pr(\delta) \cdot \sum_{b \in V} \frac{\Pr(\delta, b)}{\Pr(\delta) \cdot \Pr(b)} \\ &= \sum_{\delta \in \Delta} \Pr(\delta) \cdot \frac{1}{\Pr(\delta)} \times \sum_{b \in V} \Pr(\delta \mid b) \\ &= \sum_{b \in V} \sum_{\delta \in \Delta} \Pr(\delta \mid b) = \sum_{b \in V} 1 = |V| \end{aligned}$$

Therefore,  $C_{aj}^d$  is unbiased, as claimed.  $\square$

**5.4.1 Tipping Point.** To decide when to use partial exact computations, we use a rough estimate of the join complexity. We do so using a simple technique for join-size estimation as used by PostgreSQL.<sup>6</sup> In the case of two triple patterns  $(a_1, b_1, c_1)$  and  $(a_2, b_2, c_2)$  joining on say  $c_1 = c_2$ , the size is estimated as the product between the number of triples matched by  $(a_1, b_1, c_1)$  and  $(a_2, b_2, c_2)$ , divided by the maximum number of distinct terms of  $c_1$  or  $c_2$ . For more than two patterns, we compose the estimates in the straightforward manner. If the estimate is lower than a predefined threshold,

<sup>6</sup><https://www.postgresql.org/docs/current/static/planner-stats-details.html>

Audit Join switches to exact computation. In this case we say that the *tipping point* is reached. While simple, this join estimation allows Audit Join to consistently achieve considerable improvements, as shown in the experimental section. Investigating more sophisticated estimates (e.g., [74]) is left as an important direction for future research.

**5.4.2 Summary.** We summarize Audit Join in Figure 8. The code is similar to Section 5.4, except that it incorporates grouping. The sets  $A$  and  $B$  are projections over the attributes  $\alpha$  and  $\beta$ , respectively (Figure 5). The estimates are accumulated in  $C_a$  for every group  $a$ . The probability  $\Pr(a, b, \delta)$  corresponds to the event that the random walk starts with  $\delta$  and includes the group  $a$  and the counted value  $b$ . Hence, it is the sum of the probabilities of all such random walks. Similarly,  $\Pr(a, b)$  is the probability that the random walk includes the group  $a$  and the counted value  $b$ . Note that in line 17, the left semi-join  $G_{i+1} \times t$  consists of all the tuples of  $G_{i+1}$  that can be matched with  $t$ .

## 6 EXPERIMENTAL STUDY

Our experimental study compares the performance of our four query engine strategies: Virtuoso, Cached Trie Join (CTJ), Wander Join (WJ) and Audit Join (AJ). More specifically, in the context of answering a variety of queries in our exploration system, we address the following core questions:

- Q1: How does the performance of the two exact computation strategies – Virtuoso and CTJ – compare in the distinct case required by our system?
- Q2: How does the error rate of the two online aggregation strategies – WJ and AJ – compare over time in both the distinct and non-distinct case?

### 6.1 Implementation

We take Virtuoso as an off-the-shelf query engine and implement the other three strategies in C++. We implement WJ and CTJ as described in their corresponding papers and then implement AJ on top of these algorithms. We now discuss the configuration and implementation of each strategy.

We use Virtuoso v. 07.20.3217 [2] and configure it to use all available memory for caching indexes. Virtuoso runs the subclass closure as part of the expansion queries using property paths on the original graph; the query planner shows that this closure is executed first and takes only a few milliseconds for both knowledge bases.

Our CTJ implementation uses LFTJ [73] as the trie join algorithm. Since WJ does not support transitivity, the subclass closure is computed offline and materialized in the graph (instances are indexed with only their explicit types per the original data). The trie indexes are implemented using sorted arrays (*std::vector*) such that each search is done in  $O(\log(N))$ .

**Table 1: Dataset information**

Dataset	Version	Triples	Classes	Props
DBpedia	3.6	431,940,462	370,082	61,944
LinkedGeoData	2015-11	1,216,585,356	1,147	33,355

We implement CTJ with four of the six possible index orders:  $(s, p, o)$ ,  $(o, p, s)$ ,  $(p, s, o)$ , and  $(p, o, s)$ ; these orders are sufficient to support our exploration queries. The CTJ cache structure uses an array of hashtables (*std::unordered\_map[]*).

In WJ, the graph is saved in an unsorted array (*std::vector*). Analogously to CTJ, the subclass closure is performed offline and materialized. The algorithm uses hashtable indexes (*std::unordered\_map*) over the array that enable sampling in  $O(1)$  time. In the case of distinct – as there is no formal support for this operator in WJ – we augment it with the technique proposed by Haas et al. in Ripple Join [39, 42] for performing online aggregation in the distinct case: this technique stores the set of samples seen thus far and rejects new samples that have already been seen.

AJ is implemented on top of WJ and CTJ; it likewise assumes that the subclass closure has been materialized in the graph. Our implementation uses a hybrid hashtable/trie data-structure where the hashtable indexes point to a sorted array, allowing  $O(1)$ -time sampling for WJ and  $O(\log(n))$ -time search for CTJ. Analogously to CTJ, AJ maintains four index orders and the same caching structure. Unlike WJ, AJ uses its own unbiased estimator for distinct (per Section 5).

### 6.2 Methodology

**Data.** Our data include two large-scale knowledge graphs: DBpedia [17] and LinkedGeoData [13]; details of these two graphs are presented in Table 1. DBpedia contains multi-domain data extracted from Wikimedia projects such as Wikipedia; we take the English version of DBpedia v.3.6, which contains 400 million RDF triples, 370 thousand classes and 62 thousand properties. LinkedGeoData specializes in spatial data extracted from OpenStreetMap; we take the November 2015 version, which contains 1.2 billion RDF triples, one thousand classes, and 33 thousand properties. In the case of LinkedGeoData, since no root class is defined in the original data, we explicitly add a class that is the parent of all classes previously without a parent in the class hierarchy.

**Queries.** Our queries comprise of randomly generated exploration paths that imitate users applying incremental expansions. More specifically, our generator starts with the root class of a graph. At each step, the generator uniformly selects one of the expansion operations, which is translated to a SPARQL query of the form shown in Figure 5. Next, one of the groups (aka. bar) from the answer is randomly sampled; we apply a weighted sampling according to the size of

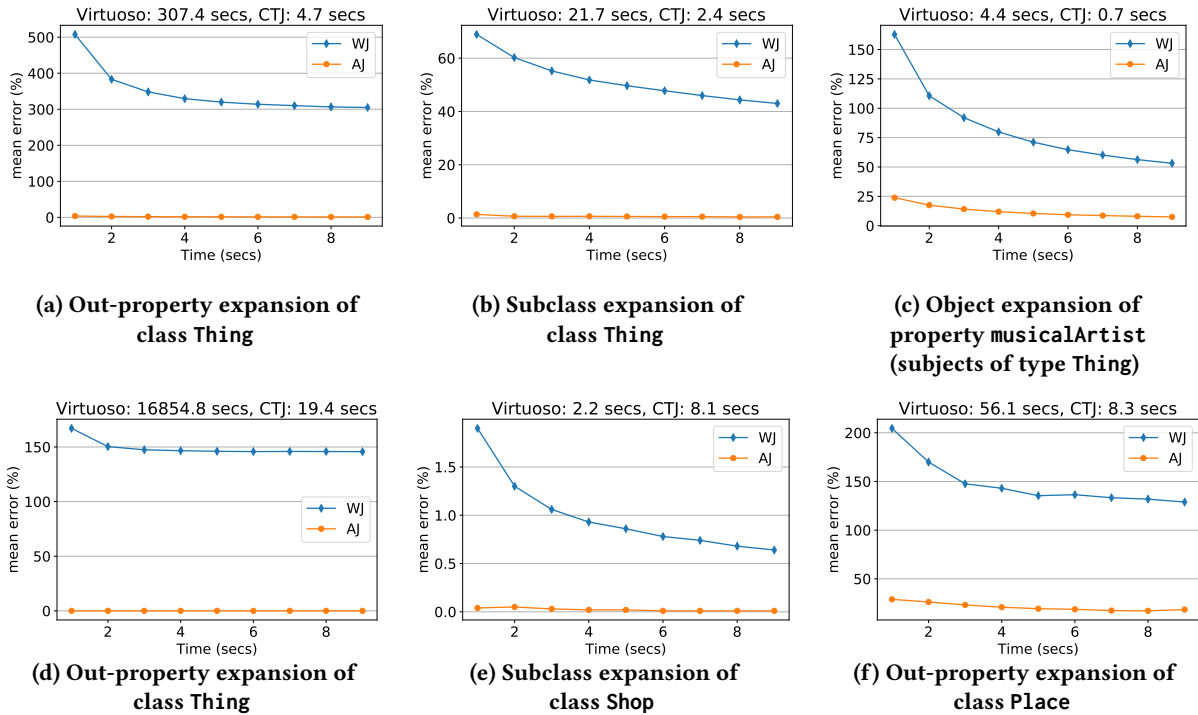


**Figure 9: The mean error per second (WJ and AJ) and exact runtimes (Virtuoso and CTJ) for a selection of six exploration queries: three from DBpedia (top) and three from LinkedGeoData (bottom)**

the group to increase focus on large groups (otherwise since the majority of groups are small, the explorations would fixate on these small groups). The generator continues for four steps or until it gets an empty result. Queries with empty results are ignored and not considered part of the path. We ran this generator 25 times for each graph resulting in a total of 33 distinct non-empty queries (listed in the appendix). The error is computed as the absolute difference between the exact count and estimated count divided by the exact result; consequently, the reported mean error is the average error over all groups in the result.

*Machine and Testing Protocol.* Our server has four 2.1 GHz Xeon E5-2683 v4 processors, 500 GB of DDR4 DRAM, and runs Ubuntu 16.04.4 Linux. Each experiment was performed three times, and the average runtime and mean error are reported. We run each online aggregation algorithm for nine seconds and report the estimation after each second. For each query, we tested different join orders of WJ and selected the one with the best mean error.

### 6.3 Results

We first present results on a selection of six queries that help demonstrate different behaviour in all four compared approaches. We then compare the error observed over time for the two online aggregation approaches over all queries,

contrasting different exploration depths, the two different datasets, and queries with and without distinct.

*Selected queries with distinct:* Figure 9 presents the results for a selection of six queries (with distinct) that illustrate a variety of behaviours in the compared approaches. Each graph presents the mean error over time, in seconds, for a specific exploration query. The times for the exact engines, specifically Virtuoso and CTJ, are indicated above the graph. The top row presents results over DBpedia, while the bottom row presents results over LinkedGeoData.

Virtuoso and CTJ take more than a second to answer most queries and take notably longer for the larger dataset: LinkedGeoData (which contains three times more edges). Focusing on Virtuoso, we see that while some queries run in the order of seconds, others run in minutes or even hours: the out-property expansion of Thing (the root class) on LinkedGeoData runs for more than four hours (see Figure 9d). On the other hand, CTJ generally offers a major performance improvement over Virtuoso: though slower in one case (see Figure 9e), in the worst cases, CTJ returns results in tens of seconds; for example, the query that took Virtuoso over 4 hours takes CTJ around 20 seconds. Still, even with the considerable performance improvements offered by CTJ, runtimes in the order of tens of seconds would hurt the interactivity and usability of our exploration system.

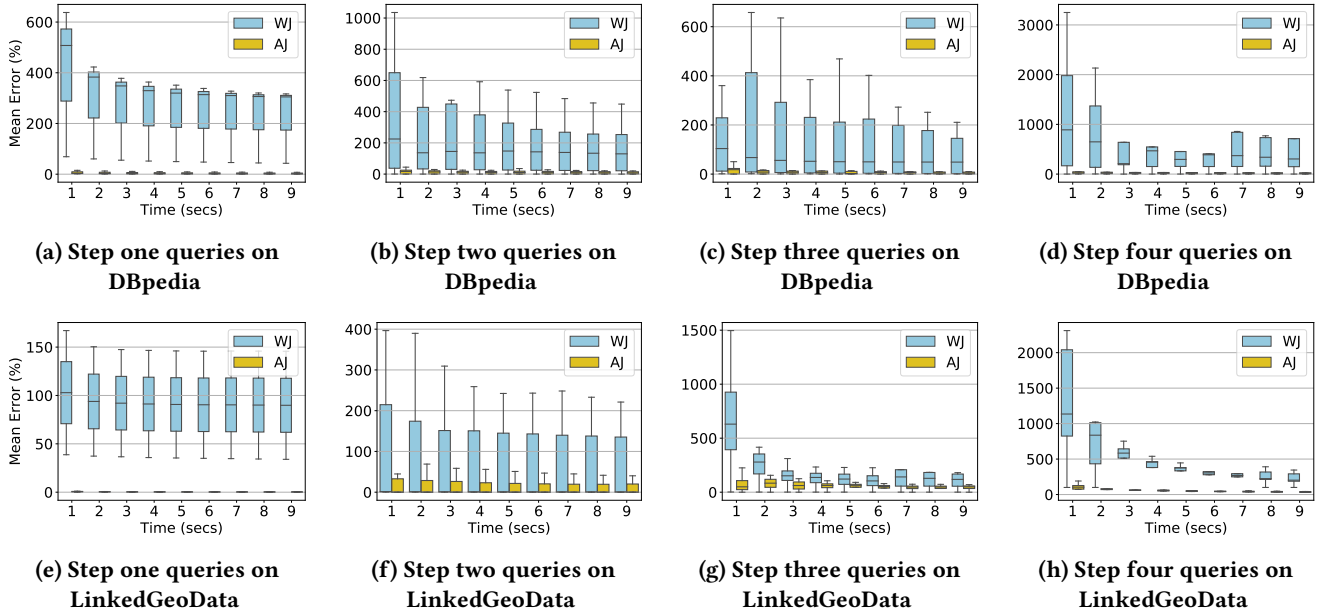


**Figure 10: Tukey plots for the mean error over time (seconds) of all queries with a varying number of exploration steps over DBpedia (top) and LinkedGeoData (bottom)**

When comparing the mean errors of WJ and AJ over time across Figure 9, it is clear that the accuracy and convergence of AJ is significantly better than WJ for the selected queries. These improvements are due to the two extensions that AJ makes over WJ: namely the reduction of rejection rates using CTJ, and the addition of an unbiased estimator for the distinct case (we shall test without distinct in later experiments). We now discuss some individual cases in more detail.

Looking first at DBpedia, for the out-property expansion of Thing (Figure 9a), the mean error of WJ is 519% after one second and 303% after nine seconds; the corresponding errors for AJ are 7.5% and 3.7%, respectively—almost two orders of magnitude improvement compared to WJ. In the object expansion of musicalArtist (Figure 9c), which originates from the subclass expansion of Thing (Figure 9b), WJ has a mean error of 163% and 53% after one and nine seconds, respectively. While still better than WJ, the accuracy of AJ drops, starting at a mean error of 24% and reaching 9% (on the other hand, given the high selectivity of the query, CTJ returns exact results in less than a second).

Moving to the second row of plots in Figure 9, while the larger size of LinkedGeoData notably affects Virtuoso and CTJ, the results for the online aggregation solutions remain similar to DBpedia. As shown in Figure 9d, WJ’s estimation of the out-property expansion on Thing results in a mean error of 167% after one second, which slowly drops to 145% after nine seconds; for the same query, AJ estimates the results with a mean error close to 0% from the first second.

The subclass expansion on Shop (Figure 9e) is quickly well-estimated by both WJ and AJ, resulting in a mean error of 1.9% and 0.04% after one second, respectively. On the other hand, estimations worsen in the third query for an out-property expansion of Place (Figure 9f); still, AJ clearly outperforms WJ in this case.

*All queries with distinct:* For each exploration depth and knowledge graph, Figure 10 presents the range of mean errors for all estimations under the distinct operator as box plots (specifically, Tukey plots), displaying the interquartile range of error (the box), the median error (the line in each box), and the most extreme data point within 1.5× the interquartile range (the whiskers). These plots show the variation of mean error across all queries with respect to time.

These results show that AJ is consistently better than WJ over all randomly generated queries: the median of mean errors for WJ in some cases reaches over 1,000% after one second and 300% after nine seconds (see Figure 10d); on the other hand, the same median errors for AJ are at worst 104% after one second, and 50% after nine seconds.

An interesting result can be found when comparing the graphs for a varying numbers of exploration steps. Taking LinkedGeoData, for example, the accuracy of WJ drops when comparing the first step (Figure 10e) with subsequent steps (Figures 10f–10h resp.). A similar trend can be seen for DBpedia (though less clear moving from step one to two). We attribute this trend to (1) an increasing number of rejections:

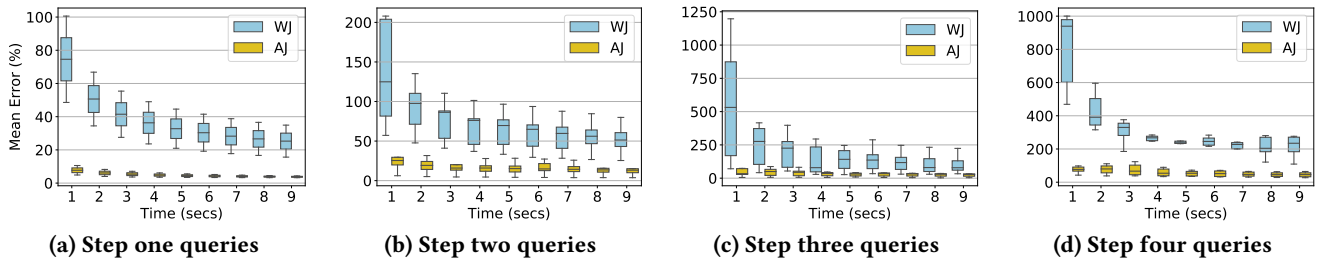


Figure 11: Error over time in seconds for queries without the distinct operator

later steps tend to become more specific, adding more selective joins; and (2) increasing duplicates: as the query becomes larger, more variables are projected away. Both issues are specifically addressed by the AJ algorithm.

*All queries without distinct:* Finally, though our exploration system requires the distinct operator for counts, we also perform experiments in the non-distinct case to understand the relative impact of the unbiased distinct estimator and the partial exact computations on reducing error in AJ. Figure 11 presents Tukey plots of mean error over time for all queries without distinct, and both datasets, separated by the number of exploration steps. Overall we conclude that: (1) the error observed for WJ drops from the distinct case to the non-distinct case; (2) the errors generally increase in AJ versus the distinct case; and (3) AJ continues to significantly outperform WJ, though by a lesser margin when considering the non-distinct case. We surmise from these results that though AJ no longer benefits from the unbiased distinct estimator, it continues to clearly outperform WJ in the non-distinct case due to the partial exact computations: the benefits of AJ are not only due to the unbiased distinct estimator.

*Summary:* Our first results show that computing exact counts for a selection of exploration queries may take in the order of hours for Virtuoso, and in the order of tens of seconds for CTJ, with both approaches slowing down for the larger LinkedGeoData graph. Though CTJ offers a major performance benefit versus Virtuoso, we conclude that computing exact results (with either approach) is not compatible with our goal of interactive runtimes. Focusing thereafter on online aggregation, we find that AJ significantly reduces error (by orders of magnitude) versus WJ over the same time period, and in most cases can quickly converge to estimates with less than 1% mean error. We also found that the performance of the online aggregation approaches is less affected by the larger size of LinkedGeoData than in the exact settings, and that the relative benefit of AJ and WJ improves as more exploration steps are added. Finally, through experiments on non-distinct queries, we find that

AJ continues to significantly reduce error versus WJ due to its inclusion of CTJ for partial exact computations.

## 7 CONCLUSIONS

We presented a formal framework for the visual exploration of knowledge graphs, where an exploration step consists of the transformation of the bar of one bar chart into the next bar chart. We also investigated the implementation of this framework using various query engines for rendering bar charts, including a SPARQL engine, a recent in-memory join algorithm, and online aggregation. Finally, we devised and analyzed Audit Join: a specialized online-aggregation algorithm that combines the random walks of Wander Join with exact computation, and extends its estimator to accommodate the count aggregations under the distinct operator. Our experiments show that the runtimes of both methods for performing exact counts are too slow for supporting interactive exploration over large-scale knowledge graphs. Focusing thereafter on online aggregation, we find that when compared with Wander Join, Audit Join significantly reduces error with respect to time in all experiments, often by orders of magnitude, including both distinct and non-distinct cases.

In terms of future directions, for one, we wish to arrive at a more general understanding of how partial exact computation complements online aggregation in order to devise a more principled way to combine both; our results show this to be a very promising approach in general, and more work can be done to refine this idea. We will also explore the application of our approach to general join queries, beyond the path queries produced by our system. We also wish to explore directions for improving the usability of our exploration system, which include: allowing to explore and contrast multiple knowledge graphs simultaneously, adding support for incremental indexing on updates, extending filtering capabilities, and adding support for further semantics beyond subclass closure. Finally, we plan to conduct user studies to increase the potential of our system for accelerating the development of applications over knowledge graphs.

## REFERENCES

- [1] Anonimized for double-blind reviewing.
- [2] Openlink Virtuoso. <https://virtuoso.openlinksw.com/>.
- [3] Sparql. <https://www.w3.org/TR/sparql11-overview/>.
- [4] Z. Abedjan, T. Grütze, A. Jentzsch, and F. Naumann. Profiling and mining RDF data with ProLOD++. In *International Conference on Data Engineering (ICDE)*, pages 1198–1201. IEEE Computer Society, 2014.
- [5] C. R. Aberger, A. Lamb, S. Tu, A. Nötzli, K. Olukotun, and C. Ré. Empty-headed: A relational engine for graph processing. *ACM Trans. Database Syst.*, 42(4):20:1–20:44, Oct. 2017.
- [6] M. Abo Khamis, H. Q. Ngo, and A. Rudra. Faq: Questions asked frequently. In *Proceedings of the 35th ACM SIGMOD-SIGACT-SIGAI Symposium on Principles of Database Systems, PODS '16*, pages 13–28, New York, NY, USA, 2016. ACM.
- [7] M. Alam, A. Buzmakov, V. Codocedo, and A. Napoli. Mining Definitions from RDF Annotations Using Formal Concept Analysis. In *International Joint Conference on Artificial Intelligence (IJCAI)*, pages 823–829. AAAI Press, 2015.
- [8] G. Aluç, O. Hartig, M. T. Özsu, and K. Daudjee. Diversified stress testing of RDF data management systems. In *International Semantic Web Conference (ISWC)*, pages 197–212, 2014.
- [9] R. Angles, M. Arenas, P. Barceló, A. Hogan, J. L. Reutter, and D. Vrgoc. Foundations of Modern Query Languages for Graph Databases. *ACM Comput. Surv.*, 50(5):68:1–68:40, 2017.
- [10] M. Arenas, B. C. Grau, E. Kharlamov, S. Marciuska, and D. Zheleznyakov. Faceted search over RDF-based knowledge graphs. *J. Web Sem.*, 37-38:55–74, 2016.
- [11] A. Aterias, M. Grohe, and D. Marx. Size bounds and query plans for relational joins. In *Proceedings of the 2008 49th Annual IEEE Symposium on Foundations of Computer Science, FOCS '08*, pages 739–748, Washington, DC, USA, 2008. IEEE Computer Society.
- [12] S. Auer, J. Demter, M. Martin, and J. Lehmann. LODStats - An Extensible Framework for High-Performance Dataset Analytics. In *Knowledge Engineering and Knowledge Management (EKAW)*, pages 353–362, 2012.
- [13] S. Auer, J. Lehmann, and S. Hellmann. Linkedgeodata: Adding a spatial dimension to the web of data. In A. Bernstein, D. R. Karger, T. Heath, L. Feigenbaum, D. Maynard, E. Motta, and K. Thirunarayan, editors, *The Semantic Web - ISWC 2009*, pages 731–746, Berlin, Heidelberg, 2009. Springer Berlin Heidelberg.
- [14] H. Bast and B. Buchhold. An index for efficient semantic full-text search. In *Conference on Information and Knowledge Management (CIKM)*, pages 369–378, 2013.
- [15] N. Bikakis, G. Papastefanatos, M. Skourla, and T. Sellis. A hierarchical aggregation framework for efficient multilevel visual exploration and analysis. *Semantic Web*, 8(1):139–179, 2017.
- [16] B. Bishop, A. Kiryakov, D. Ognyanoff, I. Peikov, Z. Tashev, and R. Velkov. Owlim: A family of scalable semantic repositories. *Semantic web*, 2(1):33–42, Jan. 2011.
- [17] C. Bizer, J. Lehmann, G. Kobilarov, S. Auer, C. Becker, R. Cyganiak, and S. Hellmann. DBpedia - a crystallization point for the web of data. *Web Semantics*, 7(3):154–165, Sept. 2009.
- [18] K. D. Bollacker, C. Evans, P. Paritosh, T. Sturge, and J. Taylor. Freebase: a collaboratively created graph database for structuring human knowledge. In *ACM SIGMOD International Conference on Management of Data (SIGMOD)*, pages 1247–1250, 2008.
- [19] J. M. Brunetti, R. G. González, and S. Auer. From overview to facets and pivoting for interactive exploration of Semantic Web data. *IJSWIS*, 9(1):1–20, 2013.
- [20] BSBM. Berlin sparql benchmark. <http://wifo5-03.informatik.uni-mannheim.de/bizer/berlinsparqlbenchmark/>.
- [21] P. Buneman and S. Staworko. RDF graph alignment with bisimulation. *PVLDB*, 9(12):1149–1160, 2016.
- [22] S. Campinas, T. Perry, D. Ceccarelli, R. Delbru, and G. Tummarello. Introducing RDF graph summary with application to assisted SPARQL formulation. In *Database and Expert Systems Applications Workshop (DEXA)*, pages 261–266. IEEE Computer Society, 2012.
- [23] S. Capadisli, S. Auer, and A. N. Ngomo. Linked SDMX data: Path to high fidelity statistical linked data. *Semantic Web*, 6(2):105–112, 2015.
- [24] Š. Čebirić, F. Goasdoué, and I. Manolescu. Query-oriented summarization of RDF graphs. *PVLDB*, 8(12):2012–2015, 2015.
- [25] Y. Chen and K. Yi. Two-level sampling for join size estimation. In *SIGMOD Conference*, pages 759–774. ACM, 2017.
- [26] M. P. Consens. Managing linked data on the web: The linkedmdb showcase. In *Latin American Web Conference (LA-WEB)*, pages 1–2, 2008.
- [27] M. P. Consens, V. Fionda, S. Khatchadourian, and G. Pirrò. S+EPPs: Construct and Explore Bisimulation Summaries, plus Optimized Navigational Queries; all on Existing SPARQL Systems. *PVLDB*, 8(12):2028–2031, 2015.
- [28] A.-S. Dadzie and M. Rowe. Approaches to visualising linked data: A survey. *Semantic Web*, 2(2):89–124, 2011.
- [29] M. d’Aquino and E. Motta. Extracting relevant questions to an RDF dataset using formal concept analysis. In *International Conference on Knowledge Capture (K-CAP)*, pages 121–128. ACM, 2011.
- [30] M. Dudás, V. Svátek, and J. Mynarz. Dataset summary visualization with lodsight. In *Extended Semantic Web Conference (ESWC) – Demo*, pages 36–40. Springer, 2015.
- [31] M. B. Ellefi, Z. Bellahsene, J. Breslin, E. Demidova, S. Dietze, J. Szymanski, and K. Todorov. RDF Dataset Profiling – a Survey of Features, Methods, Vocabularies and Applications. *Semantic Web*, 9(5):677–705, 2018.
- [32] O. Erling. Virtuoso, a Hybrid RDBMS/Graph Column Store. *IEEE Data Eng. Bull.*, 35(1):3–8, 2012.
- [33] S. Ferré. Expressive and scalable query-based faceted search over SPARQL endpoints. In *International Semantic Web Conference (ISWC)*, pages 438–453, 2014.
- [34] F. Florenzano, D. Parra, J. L. Reutter, and F. Venegas. A Visual Aide for Understanding Endpoint Data. In *International Workshop on Visualization and Interaction for Ontologies and Linked Data (VOILA@ISWC)*, pages 102–113. CEUR-WS.org, 2016.
- [35] P. Frischmuth, M. Martin, S. Tramp, T. Riechert, and S. Auer. OntoWiki – An authoring, publication and visualization interface for the Data Web. *Semantic Web*, 6(3):215–240, 2015.
- [36] A. Galakatos, A. Crotty, E. Zraggen, C. Binnig, and T. Kraska. Revisiting reuse for approximate query processing. *PVLDB*, 10(10):1142–1153, 2017.
- [37] L. González and A. Hogan. Modelling Dynamics in Semantic Web Knowledge Graphs with Formal Concept Analysis. In *World Wide Web Conference (WWW)*, pages 1175–1184, 2018.
- [38] P. J. Haas. Large-sample and deterministic confidence intervals for online aggregation. In *Proceedings of the Ninth International Conference on Scientific and Statistical Database Management, SSDBM '97*, pages 51–63, Washington, DC, USA, 1997. IEEE Computer Society.
- [39] P. J. Haas and J. M. Hellerstein. Ripple joins for online aggregation. In *Proceedings of the 1999 ACM SIGMOD International Conference on Management of Data, SIGMOD '99*, pages 287–298. ACM, 1999.
- [40] R. Hahn, C. Bizer, C. Sahnwaldt, C. Herta, S. Robinson, M. Bürgle, H. Düwiger, and U. Scheel. Faceted Wikipedia Search. In *Business Information Systems (BIS)*, pages 1–11, 2010.
- [41] P. Heim, T. Ertl, and J. Ziegler. Facet graphs: Complex semantic querying made easy. In *The Semantic Web (ESWC)*, pages 288–302, 2010.
- [42] J. M. Hellerstein, P. J. Haas, and H. J. Wang. Online aggregation. In *Proceedings of the 1997 ACM SIGMOD International Conference on Management of Data, SIGMOD '97*, pages 171–182, New York, NY, USA,

1997. ACM.
- [43] M. Hildebrand, J. van Ossenbruggen, and L. Hardman. /facet: A browser for heterogeneous Semantic Web repositories. In *International Semantic Web Conference (ISWC)*, pages 272–285, 2006.
- [44] J. Hoffart, F. M. Suchanek, K. Berberich, and G. Weikum. YAGO2: A spatially and temporally enhanced knowledge base from wikipedia. *Artif. Intell.*, 194:28–61, 2013.
- [45] D. G. Horvitz and D. J. Thompson. A generalization of sampling without replacement from a finite universe. *Journal of the American statistical Association*, 47(260):663–685, 1952.
- [46] D. F. Huynh and D. R. Karger. Parallax and companion: Set-based browsing for the data web. Technical Report. <http://davidhuynh.net/media/papers/2009/www2009-parallax.pdf>.
- [47] O. Kalinsky, Y. Etsion, and B. Kimelfeld. Flexible caching in trie joins. In *EDBT*, pages 282–293, 2017.
- [48] M. R. Kamdar, D. Zeginis, A. Hasnain, S. Decker, and H. F. Deus. RevealD: A user-driven domain-specific interactive search platform for biomedical research. *Journal of Biomedical Informatics*, 47:112–130, 2014.
- [49] S. Kinsella, U. Bojars, A. Harth, J. G. Breslin, and S. Decker. An interactive map of semantic web ontology usage. In *International Conference on Information Visualisation*, pages 179–184, 2008.
- [50] M. Kirchberg, E. Leonardi, Y. S. Tan, S. Link, R. K. L. Ko, and B. Lee. Formal Concept Discovery in Semantic Web Data. In *International Conference on Formal Concept Analysis (ICFCA)*, pages 164–179. Springer, 2012.
- [51] F. Li, B. Wu, K. Yi, and Z. Zhao. Wander join: Online aggregation via random walks. In *Proceedings of the 2016 International Conference on Management of Data, SIGMOD Conference 2016, San Francisco, CA, USA, June 26 - July 01, 2016*, pages 615–629. ACM, 2016.
- [52] E. Mäkelä, E. Hyvönen, and S. Saarela. Ontogator - A semantic view-based search engine service for web applications. In *International Semantic Web Conference (ISWC)*, pages 847–860, 2006.
- [53] N. Mihindukulasooriya, M. Poveda-Villalón, R. García-Castro, and A. Gómez-Pérez. Loupe – An Online Tool for Inspecting Datasets in the Linked Data Cloud. In *International Semantic Web Conference (ISWC) Posters & Demos*. CEUR-WS.org, 2015.
- [54] J. Moreno-Vega and A. Hogan. GraFa: Scalable Faceted Browsing for RDF Graphs. In *International Semantic Web Conference (ISWC)*, 2018.
- [55] T. Neumann and G. Weikum. Rdf-3x: A risc-style engine for rdf. *Proc. VLDB Endow.*, 1(1):647–659, Aug. 2008.
- [56] H. Q. Ngo, D. T. Nguyen, C. Re, and A. Rudra. Beyond worst-case analysis for joins with minesweeper. In *Proceedings of the 33rd ACM SIGMOD-SIGACT-SIGART Symposium on Principles of Database Systems*, PODS ’14, pages 234–245, New York, NY, USA, 2014. ACM.
- [57] H. Q. Ngo, E. Porat, C. Ré, and A. Rudra. Worst-case optimal join algorithms. *J. ACM*, 65(3):16:1–16:40, 2018.
- [58] D. Nguyen, M. Aref, M. Bravenboer, G. Kollias, H. Q. Ngo, C. Ré, and A. Rudra. Join processing for graph patterns: An old dog with new tricks. In *Proceedings of the GRADES’15, GRADES’15*, pages 2:1–2:8, New York, NY, USA, 2015. ACM.
- [59] D. T. Nguyen, M. Aref, M. Bravenboer, G. Kollias, H. Q. Ngo, C. Ré, and A. Rudra. Join processing for graph patterns: An old dog with new tricks. In *GRADES@SIGMOD/PODS*, pages 2:1–2:8. ACM, 2015.
- [60] E. Oren, R. Delbru, and S. Decker. Extending faceted navigation for RDF data. In *International Semantic Web Conference (ISWC)*, pages 559–572, 2006.
- [61] N. Pansare, V. R. Borkar, C. Jermaine, and T. Condie. Online aggregation for large mapreduce jobs. *PVLDB*, 4(11):1135–1145, 2011.
- [62] F. Picalausa, G. H. L. Fletcher, J. Hidders, and S. Vansummeren. Principles of Guarded Structural Indexing. In *International Conference on Database Theory (ICDT)*, pages 245–256. OpenProceedings.org, 2014.
- [63] R. A. A. Principe, B. Spahiu, M. Palmonari, A. Rula, F. D. Paoli, and A. Maurino. ABSTAT 1.0: Compute, Manage and Share Semantic Profiles of RDF Knowledge Graphs. In *European Semantic Web Conference (ESWC)*, pages 170–175, 2018.
- [64] C. Qin and F. Rusu. Parallel online aggregation in action. In *Conference on Scientific and Statistical Database Management, SSDBM ’13, Baltimore, MD, USA, July 29 - 31, 2013*, pages 46:1–46:4, 2013.
- [65] C. Qin and F. Rusu. PF-OLA: a high-performance framework for parallel online aggregation. *Distributed and Parallel Databases*, 32(3):337–375, 2014.
- [66] M. Rouane-Hacene, M. Huchard, A. Napoli, and P. Valtchev. Relational Concept Analysis: mining concept lattices from multi-relational data. *Ann. Math. Artif. Intell.*, 67(1):81–108, 2013.
- [67] A. Schätzle, A. Neu, G. Lausen, and M. Przyjaciel-Zablocki. Large-scale bisimulation of RDF graphs. In *Semantic Web Information Management (SWIM) Workshop*, 2013.
- [68] m. schraefel, M. Wilson, A. Russell, and D. A. Smith. mSpace: improving information access to multimedia domains with multimodal exploratory search. *Commun. ACM*, 49(4):47–49, 2006.
- [69] B. Shneiderman. The eyes have it: A task by data type taxonomy for information visualizations. In *VL*, pages 336–343, 1996.
- [70] B. B. Thompson, M. Personick, and M. Cutcher. The bigdata® RDF graph database. In *Linked Data Management*, pages 193–237. CRC Press, 2014.
- [71] Y. Tzitzikas, N. Bailly, P. Papadakos, N. Minadakis, and G. Nikitakis. Using preference-enriched faceted search for species identification. *IJMSO*, 11(3):165–179, 2016.
- [72] Y. Tzitzikas, N. Manolis, and P. Papadakos. Faceted exploration of RDF/S datasets: a survey. *J. Intell. Inf. Syst.*, 48(2):329–364, 2017.
- [73] T. L. Veldhuizen. Triejoin: A simple, worst-case optimal join algorithm. In *ICDT*, pages 96–106, 2014.
- [74] D. Vengerov, A. C. Menck, M. Zaït, and S. Chakkappen. Join size estimation subject to filter conditions. *PVLDB*, 8(12):1530–1541, 2015.
- [75] D. Vrandečić and M. Krötzsch. Wikidata: a free collaborative knowledgebase. *Commun. ACM*, 57(10):78–85, 2014.
- [76] A. Wagner, G. Ladwig, and T. Tran. Browsing-oriented semantic faceted search. In *Database and Expert Systems Applications (DEXA)*, pages 303–319, 2011.
- [77] H. Wang, Q. Liu, T. Penin, L. Fu, L. Zhang, T. Tran, Y. Yu, and Y. Pan. Semplore: A scalable IR approach to search the web of data. *J. Web Sem.*, 7(3):177–188, 2009.

## A RANDOM QUERIES

In this section, we list the queries produced by our random generator for the experiments.

### A.1 DBPedia

We use the following namespace acronyms:

- rdf: <http://www.w3.org/1999/02/22-rdf-syntax-ns>
- owl: <http://www.w3.org/2002/07/owl>
- dbo: <http://dbpedia.org/ontology>
- dbp: <http://dbpedia.org/property>
- foaf: <http://xmlns.com/foaf/0.1>
- yago: <http://dbpedia.org/class/yago>

The exploration paths are the following. Each step is a query, and we disregard duplicates of queries in our experiments.



- (1) *InProp*[owl:Thing] → *Sbj*[dbo:wikiPageRedirects]
- (2) *InProp*[owl:Thing] → *Sbj*[foaf:primaryTopic]
- (3) *OutProp*[owl:Thing] → *Obj*[dbo:musicalArtist] → *SubC*[dbo:Person] → *SubC*[dbo:Artist]
- (4) *OutProp*[owl:Thing] → *Obj*[dbo:musicalArtist] → *SubC*[dbo:Person] → *SubC*[dbo:Artist]
- (5) *OutProp*[owl:Thing] → *Obj*[rdf:type]
- (6) *SubC*[owl:Thing] → *InProp*[dbo:Agent]
- (7) *SubC*[owl:Thing] → *InProp*[dbo:TimePeriod]
- (8) *SubC*[owl:Thing] → *OutProp*[dbo:Agent]
- (9) *SubC*[owl:Thing] → *OutProp*[dbo:MeanOfTransportation] → *Obj*[dbo:length]
- (10) *SubC*[owl:Thing] → *OutProp*[dbo:Species]
- (11) *SubC*[owl:Thing] → *OutProp*[dbo:TimePeriod] → *Obj*[rdf:type]
- (12) *SubC*[owl:Thing] → *OutProp*[dbo:Work] → *Obj*[dbp:background]
- (13) *SubC*[owl:Thing] → *OutProp*[dbo:Work] → *Obj*[dbp:distributor]
- (14) *SubC*[owl:Thing] → *OutProp*[dbo:Work] → *Obj*[dbp:guests] → *SubC*[yago:Person100007846]
- (15) *SubC*[owl:Thing] → *OutProp*[dbo:Work] → *Obj*[rdf:type]
- (16) *SubC*[owl:Thing] → *SubC*[dbo:Place] → *SubC*[dbo:ArchitecturalStructure] → *OutProp*[dbo:Infrastructure]
- (17) *SubC*[owl:Thing] → *SubC*[dbo:Place] → *SubC*[dbo:NaturalPlace] → *OutProp*[dbo:Volcano]
- (18) *SubC*[owl:Thing] → *SubC*[dbo:TimePeriod]
- (19) *SubC*[owl:Thing] → *SubC*[dbo:Work] → *OutProp*[dbo:Document] → *Obj*[rdf:type]

## A.2 LinkedGeoData

We use the following namespace acronym:

- *lgdo*: <http://linkedgeodata.org/ontology/>

The exploration paths are the following. Each step is a query, and we disregard duplicates of queries in our experiments. *InProp*[·] expansions of LinkedGeoData always returned an empty result.

- (1) *OutProp*[ConnectTrees]
- (2) *SubC*[ConnectTrees] → *OutProp*[lgdo:BarrierThing]
- (3) *SubC*[ConnectTrees] → *OutProp*[lgdo:ManMadeThing]
- (4) *SubC*[ConnectTrees] → *OutProp*[lgdo:Place]
- (5) *SubC*[ConnectTrees] → *SubC*[lgdo:Amenity] → *SubC*[lgdo:Shop] → *OutProp*[lgdo:Convenience]
- (6) *SubC*[ConnectTrees] → *SubC*[lgdo:Amenity] → *SubC*[lgdo:Shop] → *OutProp*[lgdo:Craft]
- (7) *SubC*[ConnectTrees] → *SubC*[lgdo:Amenity] → *SubC*[lgdo:Shop] → *OutProp*[lgdo:Kiosk]
- (8) *SubC*[ConnectTrees] → *SubC*[lgdo:Amenity] → *SubC*[lgdo:Shop] → *OutProp*[lgdo:Pharmacy]
- (9) *SubC*[ConnectTrees] → *SubC*[lgdo:Amenity] → *SubC*[lgdo:Shop] → *OutProp*[lgdo:Supermarket]
- (10) *SubC*[ConnectTrees] → *SubC*[lgdo:BarrierThing] → *OutProp*[lgdo:Fence]
- (11) *SubC*[ConnectTrees] → *SubC*[lgdo:BarrierThing]
- (12) *SubC*[ConnectTrees] → *SubC*[lgdo:Place] → *OutProp*[lgdo:Village]
- (13) *SubC*[ConnectTrees] → *SubC*[lgdo:PowerThing]
- (14) *SubC*[ConnectTrees] → *SubC*[lgdo:RailwayThing] → *OutProp*[lgdo:BufferStop]